Academic Science Journal

Smart Drug Delivery Systems Based on Single-Wall Carbon Nanotubes Loaded with Nanocurcumin Extract for Cancer Therapy and Toxicity

Marwa R. Jwameer[*1], Sabah A. Salman[1] and Farah T. M. Noori[2]

[1] Department of Physics – College of Science, University of Diyala, Iraq
[2] Department of Physics – College of Science – University of Baghdad, Iraq

marwaphysics0@gmail.com

Received: 14 July 2022 **Accepted: 10 August 2022**

DOI: https://dx.doi.org/10.24237/ASJ.01.01.632C

Abstract

The main objective of the study is to prepare smart drug delivery systems based on single-wall carbon nanotubes. In this study, nanocurcumin (N.Cur) was loaded onto SWCNTs containing polyethylene glycol (PEG) and polyethyleneimine (PEI), which includes amino groups — this led to the successful production of PEG-PEI-SWCNTs. XRD, UV-Vis, and TEM techniques were employed to investigate the spectral and structural properties of (PEG-PEI-SWCNTs-N.Cur). The PEG-PEI-SWCNTs showed distinct crystalline structures and flaws, as well as a larger interlayer spacing, as evidenced by XRD patterns. After loading N. Cur, TEM analysis confirmed the presence of curcumin extract. UV-Vis absorbance peaks at 289, 300.98, (282,425), and (273,431) nm appear to be linked to SWCNTs, PEG-PEI-SWCNTs, N. Curcumin extract, and PEG-PEI-SWCNTs-N, respectively. After exposure to a variety of produced SWNTs and PEG-PEI-SWCNTs at concentrations ranging from 6.25 to 100 g/ml for 72 hours, the rate of growth inhibition in cancer cells including the liver cancer HepG2 cell line—was assessed. The cancer cells were found to be very dangerous by the cytotoxicity testing.

Keyword. PEGyltion, Single Wall Carbon Nano Tube, PEG 4000.

Academic Science Journal

أنظمة ذكية لتوصيل الأدوية تعتمد على أنابيب نانوية كربونية أحادية الجدار محملة بمستخلص النانو كوركومين لعلاج السرطان والسمية

مروه رشيد جوامير[1]، صباح أنور سلمان[1] و فرح طارق محمد نوري[2]

[1] قسم الفيزياء – كلية العلوم – جامعة ديالى، العراق
[2] قسم الفيزياء – كلية العلوم – جامعة بغداد، العراق

ألخلاصة

الهدف الرئيسي من الدراسة هو إعداد أنظمة ذكية لتوصيل الأدوية تعتمد على الأنابيب الكاربون النانوية أحادية الجدار. في هذه الدراسة ، تم تحميل النانو كركمين (N.Cur) على SWCNTs التي تحتوي على البولي إيثيلين جلايكول (PEG) والبولي إيثيلين أمين (PEI) ، والذي يتضمن مجموعات أمينية - أدى ذلك إلى الإنتاج الناجح لـ PEG-PEI-SWCNTs. تم استخدام تقنيات XRD و UV-Vis و TEM للتحقيق في الخصائص الطيفية والهيكلية لـ (PEG-PEI-SWCNTs-N.Cur). أظهرت PEG-PEI-SWCNTs هياكل وعيوب بلورية مميزة ، بالإضافة إلى تباعد أكبر بين الطبقات ، كما يتضح من أنماط XRD. بعد تحميل N. Cur ، أكد تحليل TEM وجود مستخلص الكركمين. يبدو أن قمم امتصاص UV-Vis عند 289 ، 300.98 ، (282.425) و (273.431) نانومتر مرتبطة بـ SWCNTs PEG-PEI-SWCNTs و N. Curcumin extract و PEG-PEI-SWCNTs-N ، على التوالي. بعد التعرض لمجموعة متنوعة من SWNTs وPEG-PEI-SWCNTs بتركيزات تتراوح من 6.25 إلى 100 جم / مل لمدة 72 ساعة، تم تقييم معدل تثبيط النمو في الخلايا السرطانية - بما في ذلك خط خلايا سرطان الكبد HepG2. تم العثور على الخلايا السرطانية لتكون خطيرة للغاية عن طريق اختبار السمية الخلوية.

الكلمة ألمفتاحية: TEM، PEGyltion، أنبوب نانو كربوني أحادي الجدار، PEG 4000.

Introduction

The second most common cause of mortality worldwide is cancer. Chemotherapy is essential for treating free cancer cells and cancer microfocuses that are difficult to detect. Chemotherapy employs chemicals to either eradicate or stop the spread of cancer cells [1]. however, the development of smart nanocarrier-based drug delivery systems, also known as Smart Drug Delivery Systems (SDDSs), was prompted by the limits of conventional chemotherapy [2].SDDSs are a type of drug delivery system that can autonomously relay a signal, respond,

administer the medicine, and cease distributing the drug. All types of SDSS have the same goal: to administer an expected quantity of medicine at an expected time and appropriate location. SDDS control signals include exterior signals such as various wavelengths of light, magnetic fields, electric fields, and ultrasound, as well as interior signals such as redox, pH, concentrations of particular biomolecules, and enzyme activity. SDDSs are built on the foundation of carriers [3], which include (i) liposomes, (ii) micelles, (iii) dendrimers, (iv) mesoporous silica nanoparticles (MSNs), (v) gold nanoparticles (GNPs), (vi) super paramagnetic iron oxide nanoparticles (SPIONs), and (vii) carbon nanotubes (CNTs). SDDSs identify cancer locations by comparing physiochemical changes between healthy cells and cancer cells. Passive and aggressive targeting are the two main methods for precisely locating the cancer cell site [4]. As noted above, one of the most promising smart delivery mechanisms for drugs is the use of carbon nanotubes (CNTs).

The transport of bioactive molecules, such as medicines, targeted cancer therapy, and biological imaging are just a few biomedical applications that have generated a lot of interest in these structures. This is due to their special qualities, which include their broad surface area, low density, excellent stability, and other innate mechanical, optical, and electrical characteristics [5-7].

Single-walled CNTs (SWCNTs) and multi-walled CNTs (MWCNTs) are two different types of CNTs that can be manufactured [8]. The synthesis of SWCNTs is simple, and they rapidly cross biological barriers [9]. Single-wall carbon nanotube (SWCNTs) functionalization is primarily used to enhance the physical characteristics of SWCNTs, such as their solubility and dispersity, as well as their bio-performance. SWCNTs may be more detrimental to the body if they have poor dispersion and significant agglomeration [10]. Thus, surface functionalization is an ideal strategy to minimize SWCNT cytotoxicity via effective cellular absorption mechanisms. Furthermore, SWCNT functionalization has a direct impact on cellular uptake quality as well as cellular internalization. Previous studies have shown that curcumin may suppress the development of a range of tumor cells, promote cell differentiation, and trigger death in some cancers. Curcumin's cytotoxicity is based on the inhibition of several cellular signal transduction pathways that play a key role in cell growth, differentiation, and malignant

transformation [11]. In spite of this, CNTs have only found limited practical use because of a number of drawbacks, including as high hydrophobicity and rapid aggregation in aqueous conditions, both of which are connected to cytotoxicity and other negative biological effects [12]. There have been several attempts and efforts to enhance CNTs' dispersibility in water and minimize their aggregation [13,14]. Of these, noncovalent coating with hydrophilic carboxylic acid groups by oxidizing acid treatment is the most frequently employed method [15,16].

Polyethylene glycol (PEG) and polyethyleneimine (PEI), which contain amino groups, were used in this study to conjugate SWCNTs. This process was performed by using EDC hydrochloride ($C_6H_{17}N_3$–HCl) and a catalyst (N hydroxysuccinimide) to cause esterification between SWCNTs, PEG, and PEI to form PEG-PEI-SWCNTs. The SWCNTs were initially cut by ultrasonic scission in a number of potent acid solutions to increase dispersion in water. The CNTs were then functionalized by grafting PEG and PEI onto them; this was done in an effort to improve tumor site targeting while reducing premature nanocarrier removal and loss. The nanocurcumin-loaded PEG-PEI-SWCNTs (i.e., PEG-PEI-SWCNTs-N.Cur) were obtained by loading the PEG-PEI-SWCNTs through π-stacking; these structures were then characterized using X-ray diffraction (XRD), UV-Vis spectroscopy, Raman spectroscopy, and transmission electron microscopy (TEM).

Experimental Section

Chemical Material

In terms of materials used in this study, 99% SWCNTs, 32% HNO_3, 37.5%, EDC hydrochloride ($C_8H_{17}N_3$-HCl), and 98% N-Hydroxysuccinimide (NHS) were obtained from Sigma-Aldrich. H_2SO_4 at 98% was acquired from LOBA Chemie. PEG 4000 was purchased from HI Media, whereas PEI was acquired from Sigma-Aldrich. Trypsin/EDTA, Fetal bovine, and RPMI 1640 serum were supplied by Capricorn (Germany). Santacruz Biotechnology (USA), Bio-World (USA), and Nanochemazone (USA) were used for the purchases of DMSO, MTT stain, and 99% curcumin (Cur) (Canada).

Preparation of PEG 4000 - PEI Functionalized SWCNTs

To prepare the PEG-PEI-SWCNTs, we mixed 0.4 g of SWCNTs in a 1:1 mixture of sulfuric and nitric acid on an electromagnetic mixer for two hours without heating. After mixing, the product was filtered using filter paper and washed with ionic water and methanol, and then precipitated to yield powder. We then poured 120 mL of ionic water into another beaker, added 6.2 g of EDC-HCL and 3.5 g of NHS material, and set it on the electromagnetic mixer for half an hour to dissolve the substances in the ionic water; after half an hour, we added SWCNTs to form the SWCNTs-COOH stage. After progressively adding 96 g of PEG-4000 and 8 g of PEI and mixing on the electromagnetic mixer for 24 hours, the solution was then put into a Petri dish and set in an electric oven at a temperature of 80 °C to dry. The result was a paste-like substance with a sticky texture, indicating its high viscosity, which was then stored in a glass box until required.

Loading Nanocurcumin on PEG-PEI-SWCNTs

For loading Cur onto the PEG-PEI-SWCNTs, 2.250 mL of the Cur solution (3.33 mg/mL concentration) was added to 7 mL of aqueous PEG-PEI-SWCNTs suspension (4.28 mg/mL concentration) and stirred overnight. The ratio of Cur to PEG-PEI-SWCNTs was approximately 1:4. To get the final sample, which is known as curcumin-bound PEG-PEI-SWCNTs (i.e., PEG-PEI-SWCNTs-N.Cur), the suspension was centrifuged at 12,000 rpm at 25 °C for 150 minutes and dried for 48 hours at 40 °C in an oven.

$$\boldsymbol{drug\ loading\ content}(\%) = \frac{\boldsymbol{weight\ of\ drug\ in\ nanoparticles}}{\boldsymbol{weight\ of\ nanoparticles}} \times \mathbf{100} \quad \text{.....(1)}$$

Bio Activity of PEG-PEI-SWCNTs-N.Cur

Anticancer activity

Cell Cultures Maintenance

The RPMI-1640 medium was supplemented with 10% fetal bovine serum, 100 units/mL penicillin, and 100 g/mL streptomycin to maintain AMJ13 and HepG2 cells.After being reseeded at 80% confluence and cultured at 37 °C, the cells were passaged twice weekly with Trypsin-EDTA.

Cytotoxicity Assays

Using 96-well plates, an MTT test was carried out to investigate the cytotoxic impact of CNTS and PEG-CNTs with the cell lines seeded at a density of 1,104 cells per well. After 24 hours or when a confluent monolayer was reached, the cells were exposed to various concentrations of the tested substances. By removing the media, adding 28 L of a 2 mg/mL MTT solution, and incubating the cells for 2.5 hours at 37 °C after 72 hours of treatment, cell viability was assessed. After the MTT solution was removed from the wells, the crystals in the wells were made soluble by adding 130 L of DMSO (Dimethyl Sulphoxide) and shaking the mixture for 15 minutes at 37 °C. A microplate reader was used to measure the absorbency at 492 nm, and the experiment was carried out three times. The percentage of cytotoxicity, or the rate of cell growth inhibition, was calculated using the equation shown below:

$$\boldsymbol{Inhibition\ rate\ =\ A-\ B/A\ *\ 100} \quad \textbf{.....(2)}$$

where A represents the control's optical density and B denotes the samples' optical density.

At a density of 1,105 cells per mL, the cells were seeded into 24-well micro-titration plates and cultivated for 24 hours at 37 °C to observe their form under an inverted microscope. After that, they received a 24-hour treatment with CNTs or PEG-CNTs at IC50. The plates were exposed, then dyed with crystal violet stain, and heated at 37 °C for 10 to 15 minutes. It took several gentle washes with tap water to thoroughly remove the color off the spot. A digital camera attached to the microscope was used to take pictures as the cells were viewed under an inverted microscope at a 40× magnification.

Statistical analysis:

GraphPad Prism 6 was used to statistically evaluate the data acquired using an unpaired t-test. The results of three replicate measurements were represented as the mean and standard deviation.

Results and discussion

Physical Characterization of (PEG-PEI-SWCNTs-N.Cur)

The PEG-PEI-SWCNTs-N.Cur were characterized by UV-Vis spectroscopy, XRD and TEM. The bonding and structure of PEG-PEI-SWCNTs-N.Cur, as well as a straightforward schematic of their synthesis.

Optical Properties of PEG-PEI-SWCNTs-N.Cur

In the UV-vis spectra of SWCNTs and PEG-PEI-SWCNTs (Figure 2), the black line at 289 nm represents the absorption bands that relate to the π–π* electronic transition for C-C (aromatic rings) and n–π* transition for C=O in the SWCNTs. The green line at 300.98 nm indicates a shift of these transitions, which confirms the synthesis of PEG-PEI-SWCNTs [17-20]. The blue line illustrates the spectra of N.Cur and the orange line represented PEG-PEI-SWCNT-N. Cur. The Cur spectrum includes two peaks at 275 nm and 425 nm. In UV-Vis spectra, the highest absorption peak for Cur is 420–430 nm; in our data, an absorption peak at 431 nm occurs in the UV-Vis spectra, which is typical of Cur, implying binding of Cur to PEG-PEI-SWCNTs. When compared to Cur suspension, the most plausible explanation is π–π* interaction between Cur and PEG-PEI-SWCNTs; in addition, the change in curcumin maximum absorption might be potentially related to its interaction with the more soluble co-polymer [21-23].

Academic Science Journal

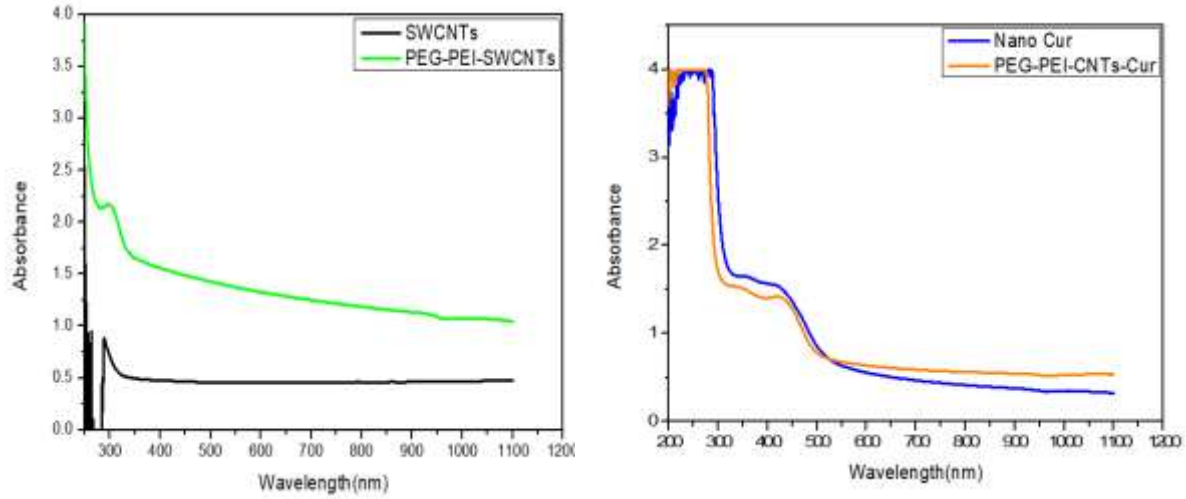

A-SWCNTs, PEG-PEI-SWCNTs **B-N.Cur, PEG-PEI-SWCNTs-**

Figure 2: UV – Vis spectrum for SWCNTs, PEG-PEI-SWCNTs, N.Cur, PEG-PEI-SWCNTs-N.Cur.

Structural Properties of PEG-PEI-SWCNTs-N.Cur

The XRD pattern of the SWCNTs is depicted by the black line in Figure 3. A prominent peak is visible at 2θ = 25.6299° in relation to the (002) peak with a d-spacing value of 3.4729 Å which complies with the hexagonal shape of single-wall carbon nanotubes. The functionalization of PEG-PEI-SWCNTs-N.Cur is represented by the orange line with a broad peak at 2θ = 23.33° and a d-spacing value of 4.63888 Å. This peak results from functionalized groups, however, the peak correlating to the SWCNTs disappears. This result is caused by SWCNTs' impact on the PEG and PEI molecular chains' structure, which alters the crystal lattice's crystallization sequence. As a result, PEG-PEI loses some of its crystallinity, making it easier for PEG-PEI to effectively attach to the nanotubes of SWCNTs [12,17,18]. The orientation (002) was determined using High Score Plus XRD analysis software. The values of the crystalline size for the SWCNTs and PEG-PEI-SWCNTs-N.Cur were equal to 3 nm and 7.58 nm, respectively [17].

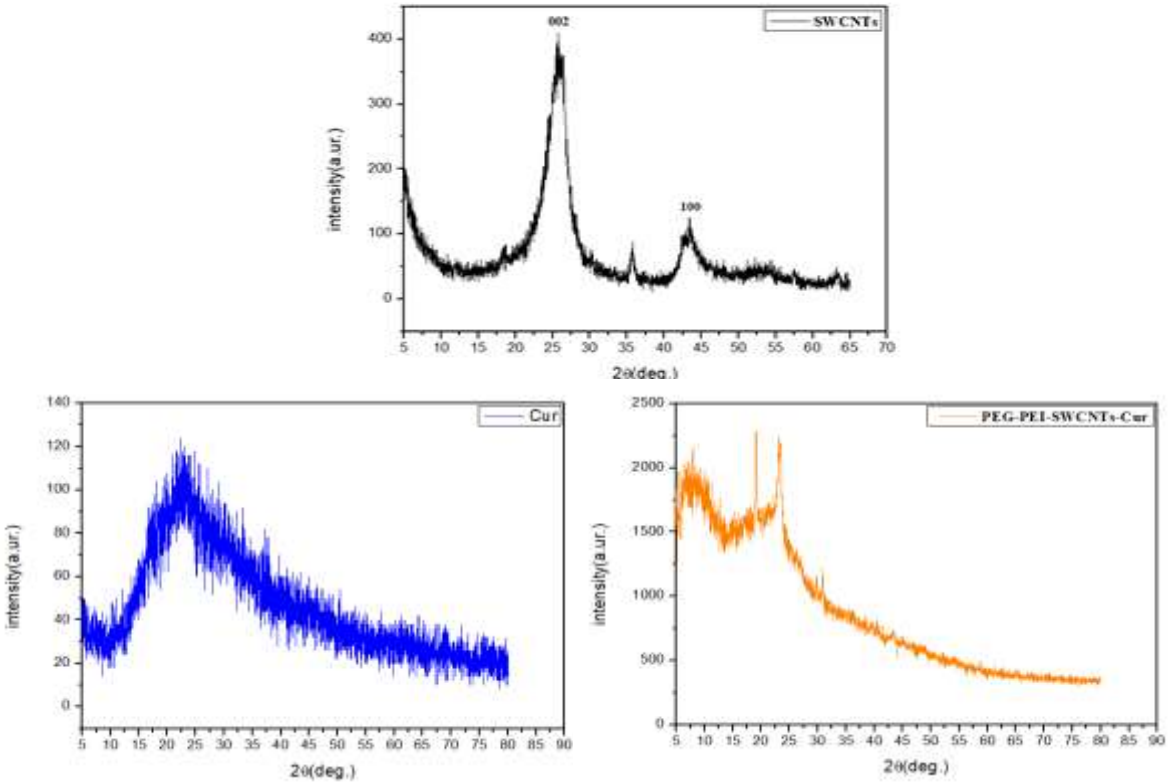

Figure 3: The XRD pattern for SWCNTs, Cur, PEG-PEI-SWCNTs- N.Cur.

Morphological Properties of PEG-PEI-SWCNTs- N.Cur

TEM analysis

TEM was used to examine the morphology of SWCNTs and PEG-PEI-SWCNTs. Figure 4 displays the TEM images of the condensed and functionalized SWCNTs. According to TEM images, unprocessed SWCNTs are long, curving aggregates that resemble bundles of inhomogeneous aggregates made up of several tubes (Figure 4-a).

Raw and acid-treated SWCNTs differ noticeably in terms of length and dispersion condition. Following acid treatment, the short SWCNTs show reduced tube lengths, with the tubular endocytosis of nanotubes facilitated by structures with hollow lumens. There is no obvious difference in the morphological characteristics of the CNTs-COOH produced with different acid solutions; they are all distributed into single tubes with smooth surfaces and no signs of

aggregation. PEG-PEI-SWCNTs are rough, tubular structures, and some of the particles appear to be linked and scattered along the sidewalls of the nanotubes, which may suggest the conjugation of PEG and PEI groups to the nanotubes [12]. The N. Cur nanoparticles showed an average size of 30 nm along with spherical morphology and low polydispersity, while the designed drug of PEG-PEI-SWCNTs-N.Cur showed conjugated polymers with N.Cur [24,25]. This link between SWCNTs, PEG, PEI, and N.Cur is attributed to the fact that carbon nanotubes have superior electrical conductivity, and will therefore act as magnetic poles that attract the rest of the molecules around it, thus, the structure will be as shown in Figure 4-C.

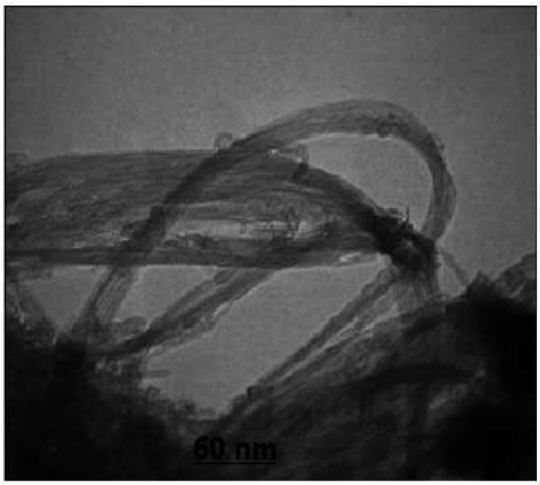

(a) SWCNTs 60nm

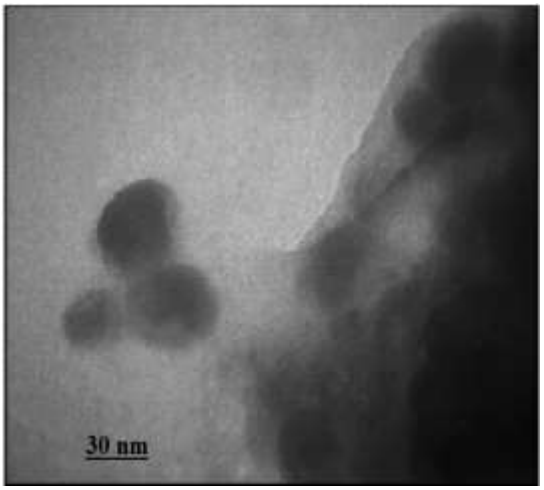

(B) Nano Curcumin 30 nm

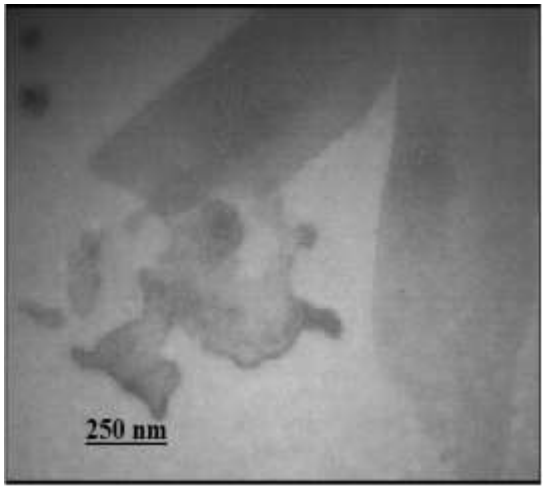

(C) PEG-PEI-SWCNTs-N. Cur 250nm

Figure 4:TEM images of (A)SWCNTs, (B)N.Cur, (C) PEG-PEI-SWCNTs-N.Cur

Anti-Proliferative Activity of CNTs and PEG-PEI-SWCNTs-N.Cur

Anti-Proliferative Activity of (SWCNTs, PEG-PEI-SWCNTs-N.Cur) Against Cancer Cell Line

In order to demonstrate the efficacy of these compounds in eliminating infected cells at a range of doses ranging between 6.26 and 100 mg/ml, the cytotoxic effect of SWCNTs, PEG-PEI-SWCNTs, and PEG-PEI-SWCNTs-N.Cur on Hep G2 cells was examined, as shown in Figures 5-a, b, and c. These substances show killing activity for the cells under study, with effectiveness increasing with increased concentration of the SWCNTs, PEG-PEI-SWCNTs, and PEG-PEI-SWCNTs. Based on Figure 5-a, we note that 57.5% of the HepG2 cells were killed with a concentration of 100 µg/ml of SWCNTs. Figure 6-b demonstrates that when PEG-PEI-SWCNTs were used at a concentration of 100 g/ml, 74 percent of the Hep G2 cells were destroyed, while 87.5% of the Hep G2 cells were killed at a concentration of 100 g/ml PEG-PEI-SWCNTs-N.Cur (Figure 5-c). Through morphological alterations in Hep G2 cell lines, the characteristics of apoptosis were also investigated. The treated cells retained their original morphological forms, as shown by the control cells. However, both cell lines showed morphological alterations when treated with SWCNTs, PEG-PEI-SWCNTs, and PEG-PEI-SWCNTs-N.Cur. Figure 5 show that those treated with the SWCNTs, PEG-PEI-SWCNTs, and PEG-PEI-SWCNTs-N.Cur had lower toxicity, owing to a decrease in the number of HepG2 cell colonies, indicating significant cell-killing activity [26,27]. Because nanoparticles have a synergistic impact at high concentrations, their effect is larger than that at lower concentrations, as evidenced by variations in shape, loss of interaction with surrounding cells, and a decrease in cell density as concentrations increase throughout treatment [27]. We observe that the rate of cell killing with PEG-PEI-SWCNTs for both types of cancer cells is higher than that with

SWCNTs alone (Figure 5-b). This could be as a result of the PEG being grafted onto the SWCNTs, which led to the formation of an efficient electrostatic layer in solution. Alternatively, this effect can be explained by PEG enhancing the dispersion of SWCNTs. Gravity and van der Waals forces are overcome by the SWCNTs' anti-static force, increasing water solubility. This result suggests that SWCNTs are more biocompatible after having PEG applied to their surfaces. This could be as a result of PEG's non-toxic, non-antigenic, and non-immunogenic properties, as well as its distinctive physicochemical properties and high biocompatibility. As a result, SWCNTs as a functional group are altered when PEG is used [28]. The biocompatibility of the materials for a range of biomedical applications can also be greatly enhanced by chemically altering PEI to change the surface charges and cytotoxicity of SWCNTs [29]. This alteration is brought on by the ammonium (NH_4^+) ions present in PEI polymers, which have a high positive charge density. Because PEI polymers have a significant electrostatic affinity for polynuclear acids, they are frequently employed as coating materials for inorganic nanoparticles and polymeric carriers for gene delivery. After intracellular uptake, they also exhibit an endosomal escape ability via the "proton sponge" function [30], which increases the lethal effect on cells and extends the drug's release duration. According to Figure 6-c, PEG-PEI-SWCNTs-N.Cur kills cancer cells more quickly than SWCNTs and PEG-PEI-SWCNTs. This is true for both types of cancer cells. This outcome might be related to the loading of nanocurcumin onto PEG-PEI-SWCNTs, which improves the efficacy and bioavailability of these compounds as anticancer agents. This also results in the loaded medication being more soluble and having improved stability (i.e., nanocurcumin). Overall, because they have a reduced risk of toxicity than other polymers, biocompatible and biodegradable materials are perfect for use in drug delivery systems [32,33].

Academic Science Journal

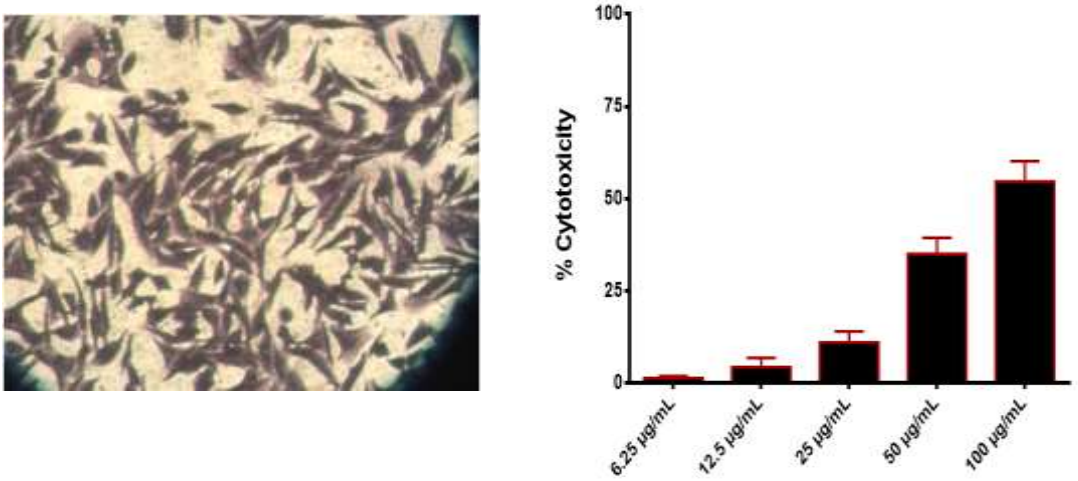

A-SWCNTs

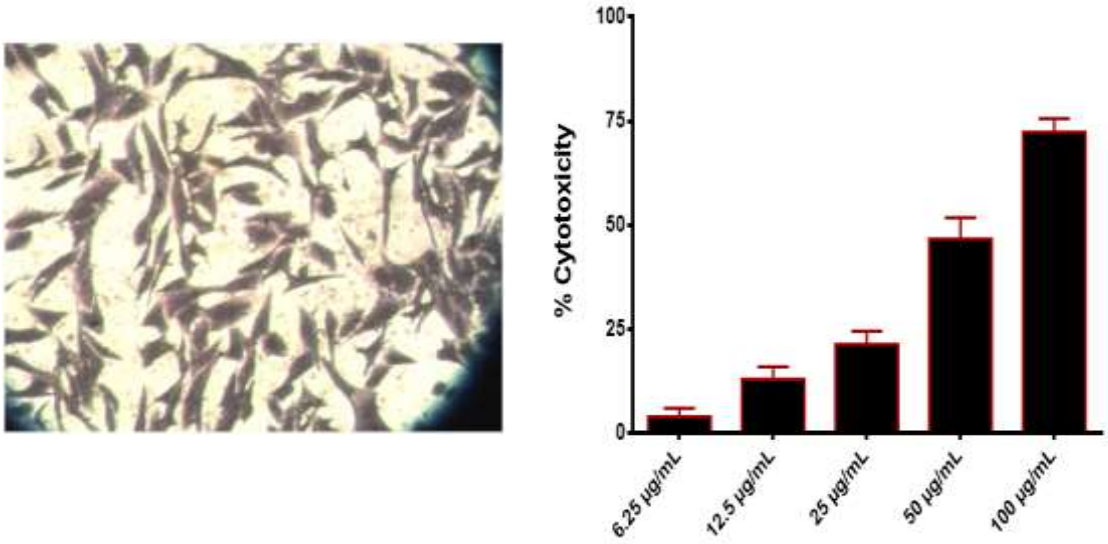

B-PEG-PEI-SWCNTs

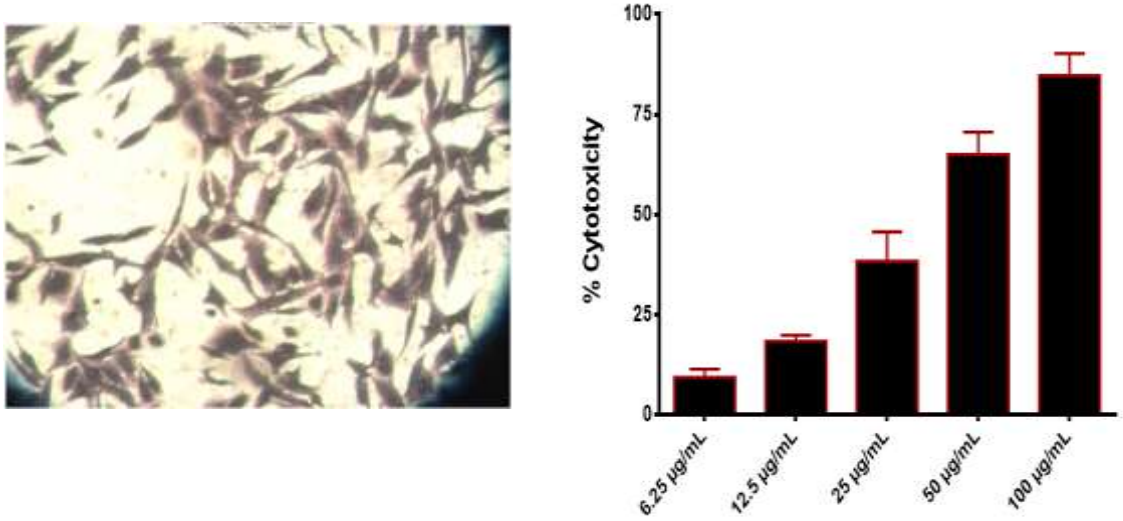

C-PEG-PEI-SWCNTS-N.Cur

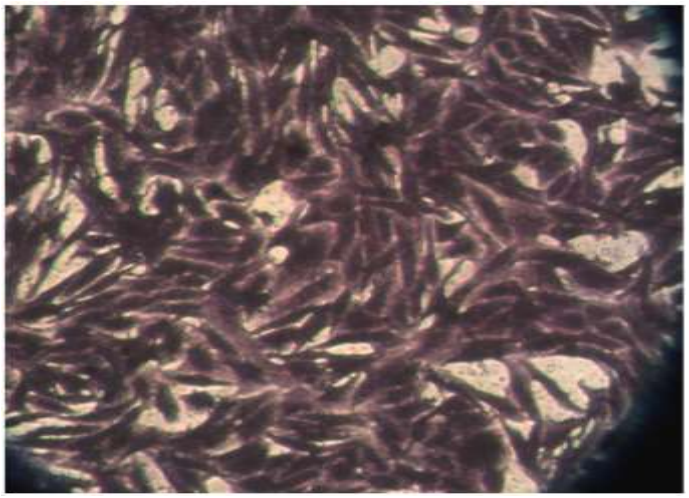

D- Control untreated HepG2 cells

Figure 5: Cytotoxic effect and Morphological changes of (A-SWCNTs, B-PEG-PEI-CNTs, C-PEG-PEI-SWCNTs- N.Cur, D- Control untreated) in HepG2 cells

Conclusions

In this study, we investigated the anticancer activity of functionalized single-wall carbon nanotubes with PEG-PEI and loading of nanocurcumin. Using PEG and the amino group-containing polyethyleneimine (PEI), we conjugated SWCNTs with PEI to create PEG-PEI-

SWCNTs. To enhance their dispersion in water, the SWCNTs were first ultrasonically cut to a shorter length in several strong acid solutions. After that, the SWCNTs were grafted with PEG and PEI. The goal of this functionalization was to decrease premature removal and loss of nanocarriers, enhance tumor site targeting, and eventually enhance the efficacy of the PEG-PEI-SWCNTs' smart drug delivery. The PEG-PEI-SWCNTs were then loaded with nanocurcumin to obtain PEG-PEI-SWCNTs-N.Cur. From the results, the drug-loaded PEG-PEI-SWCNTs-N.Cur showed greater inhibitory activity than the SWCNTs and PEG-PEI-SWCNTs. Our study demonstrated that the preparation and characterization of the SWCNTs, nanoparticle-functionalized PEG-PEI-SWCNTs, and drug-loaded PEG-PEI-SWCNTs-N.Cur was successful and demonstrated potential anticancer activity against HepG2 liver cancer cell lines.

References

1. S. Hossen, M. K. Hossain, M. K. Basher, M. N. H. Mia, M. T. Rahman, M. J. Uddin, Journal of advanced research, 15, pp.1-18(2019)
2. K. Nooter, G. Stoter, Pathology-Research and Practice, 192(7), 768-780(1996)
3. H. Zhang, T. Fan, W. Chen, Y. Li, B. Wang, , Bioactive Materials, 5(4), 1071-1086(2020)
4. Y. Matsumura, H. Maeda, Cancer research, 46(12 Part 1), 6387-6392(1986)
5. K. Bates, K. Kostarelos, Advanced drug delivery reviews, 65(15), 2023-2033(2013)
6. H. Gong, R. Peng, Z. Liu, Advanced drug delivery reviews, 65(15), 1951-1963(2013)
7. B. S. Wong, S. L. Yoong, A. Jagusiak, T. Panczyk, H. K. Ho, W. H. Ang, G. Pastorin, Advanced drug delivery reviews, 65(15), 1964-2015(2013)
8. N. Pippa, D. D. Chronopoulos, D. Stellas, R. Fernández-Pacheco, R. Arenal, C. Demetzos, N. Tagmatarchis, International journal of pharmaceutics, 528(1-2), pp.429-439(2017)
9. S. Prakash, M. Malhotra, W. Shao, C. Tomaro-Duchesneau, S. Abbasi, Advanced drug delivery reviews, 63(14-15), 1340-1351(2011)
10. H. Wu, H. Shi, H. Zhang, X. Wang, Y. Yang, C. Yu, C. Hao, J. Du, H. Hu, S. Yang, Biomaterials, 35(20), 5369-5380(2014)
11. F. Karchemski, D. Zucker, Y. Barenholz, O. Regev, Journal of controlled release, 160(2), 339-345(2012)
12. S.Yang, Z. Wang, Y. Ping, Y. Miao, Y. Xiao, L. Qu, L. Zhang, Y. Hu, J. Wang, , Beilstein Journal of Nanotechnology, 11(1), 1728-1741(2020)
13. A. Battigelli, C. Ménard-Moyon, T. Da Ros, M. Prato, A. Bianco, Advanced drug delivery reviews, 65(15), 1899-1920(2013)
14. V. Rastogi, P1. Yadav, S. S. Bhattacharya, A. K. Mishra, N. Verma, A. Verma, J. K. Pandit, 1-23(2014)

15. H. He, L. A. Pham-Huy, P. Dramou, D. Xiao, P. Zuo, C. Pham-Huy, BioMed research international, (2013)
16. S. Vardharajula, S. Z. Ali, P. M. Tiwari, E. Eroğlu, K. Vig, V. A. Dennis, S. R. Singh, International journal of nanomedicine, 7, 5361(2012)
17. V. Mishra, P. Kesharwani, N. K. Jain, Critical Reviews™ in Therapeutic Drug Carrier Systems, 35(4),(2018)
18. M. Jwameer, F. Noori, S. Anwer, Journal of Mechanical Engineering Research and Development, 44 (10) , 44-56(2021)
19. M. A. Jihad, F. Noori, M. S. Jabir, S. Albukhaty, F. A. AlMalki, A. A. Alyamani, Molecules, 26(11), 3067(2021)
20. J. Charmi, H. Nosrati, J. M. Amjad, R. Mohammadkhani, H. Danafar, Heliyon, 5(4), e01466(2019)
21. Y. Wang, G. Sun, Y. Gong, Y. Zhang, X. Liang, L. Yang, Nanoscale research letters, 15(1), 1-11(2020)
22. E. Pinilla-Peñalver, M. L. Soriano, G. M. Durán, E. J. Llorent-Martínez, A. M. Contento, Á. Ríos, Microchimica Acta, 187(8), 1-11(2020)
23. T. A. Nguyen, Q. D. Tang, D. C. T. Doan, M. C. Dang, Advances in Natural Sciences: Nanoscience and Nanotechnology, 7(3), 035003(2016)
24. A. Jorio, R. Saito, J. H. Hafner, C. M. Lieber, D. M. Hunter, T. McClure, G. Dresselhaus, M. S. Dresselhaus, Physical Review Letters, 86(6), 1118(2001)
25. P. Kushwaha, A. Yadav, M. Samim, S. J. S. Flora, Chemico-biological interactions, 286, 78-87(2018)
26. N. H. Ali, A. M. Mohammed, Biotechnology Reports, 30, e00635(2021)
27. K. S. Khashan, F. A. Abdulameer, M. S. Jabir, A.A. Hadi, , G. M. Sulaiman, Advances in Natural Sciences: Nanoscience and Nanotechnology, 11(3), 035010(2020)
28. S. Yu, Y. Zhang, L. Chen, Q. Li, J. Du, Y. Gao, L. Zhang, Y. Yang, Experimental and therapeutic medicine, 16(2), 1103-1110(2018)
29. M. Shen, S. H. Wang, X. Shi, X. Chen, Q. Huang, E. J. Petersen, R. A. Pinto, J. R. Baker Jr, W.J. Weber Jr, The Journal of Physical Chemistry C, 113(8), 3150-3156(2009)
30. Y. K. Buchman, E. Lellouche, S. Zigdon, M. Bechor, S. Michaeli, J.P. Lellouche, Bioconjugate chemistry, 24(12), 2076-2087(2013)
31. Y. Hailing, L. Xiufang, W. Lili, L. Baoqiang, H. Kaichen, H. Yongquan, Z. Qianqian, M. Chaoming, R. Xiaoshuai, Z. Rui, L. Hui, Nanoscale, 12(33), 17222-17237(2020)
32. B.M. Tahmasebi, M.V. Erfani, E. Babaei, F. Najafi, M. Zamani, M. Shariati, S. Nazem, B. Farhangi, P. Motahari, M. Sadeghizadeh, Progress in Biological Sciences , 5(2), 143-158(2015)
33. A. Baldi, A. De Luca, P. Maiorano, C. D'Angelo, A. Giordano, International journal of molecular sciences, 21(5), 1839(2020)